



Harnessing complexity: integrating remote sensing and fuzzy expert system for evaluating land use land cover changes and identifying mangrove forest vulnerability in Bangladesh

Md. Monirul Islam^{1,2} · Dewan Abdullah Al Rafi³ · Arifa Jannat^{4,5} · Kentaka Aruga⁶ · Sabine Liebenehm⁷ · Radita Hossain⁸

Received: 30 April 2024 / Revised: 7 August 2024 / Accepted: 28 December 2024
© The Author(s) 2025

Abstract

Purpose: This study analyzes Landsat images to examine the alterations in land cover within the Sundarbans and its surrounding regions in Bangladesh, spanning twenty-one years from 2000 to 2021. Furthermore, we develop a mangrove vulnerability map considering the combined effect of eight socioeconomic, geophysical, and climatic factors. **Methods:** Land use land cover (LULC) changes in the study area over a 21-year period were assessed using a random forest model, and the vulnerability analysis employed a fuzzy expert-based multicriteria decision-making (MCDM) approach. **Results:** The results show that a significant portion of the mangrove forest has been transformed into aquaculture practices because of the expansion of high-value shrimp cultivation. A decrease in forest areas and the expansion of aquaculture zones suggest a livelihood shift among the local population over time. This transition has adversely affected human activities within the ecosystem and the biodiversity of mangrove forests. Consequently, it is imperative to implement suitable measures to enhance the state of mangrove forests and safeguard their biodiversity. The vulnerability analysis shows that the highly vulnerable, moderately vulnerable, and low vulnerable areas cover 35.66%, 26.86%, and 19.42%, respectively. **Conclusion:** The vulnerability maps generated in this research could serve as a valuable resource for coastal planners seeking to ensure the sustainable stewardship of these coastal mangrove forests. These results offer a detailed understanding of coastal mangrove LULC patterns and vulnerability status, which will be useful for policymakers and resource managers to urgently incorporate into coastal land use and environmental management practices.

Keywords LULC · Change detection · Vulnerability assessment · Fuzzy-logic approach · Remote sensing & GIS · Random forest

Md. Monirul Islam
monir96@bau.edu.bd

¹ Department of Agricultural Economics, Bangladesh Agricultural University, Mymensingh, Bangladesh

² Commonwealth Scientific and Industrial Research Organisation - CSIRO, Waite Campus, Adelaide, South Australia, Australia

³ Department of Agricultural and Applied Economics, The University of Georgia, Georgia, USA

⁴ Institute of Agribusiness and Development Studies, Bangladesh Agricultural University, Mymensingh, Bangladesh

⁵ School of Agriculture, Food and Wine, University of Adelaide, Urrbrae, South Australia, Australia

⁶ Graduate School of Humanities and Social Sciences, Saitama University, Saitama, Japan

⁷ Department of Agricultural and Resource Economics, Department of Economics, University of Saskatchewan, Saskatoon, Saskatchewan, Canada

⁸ Department of Mathematics, The University of Louisiana, Lafayette, USA

Introduction

The transformation of land use land cover (LULC) changes driven by rapid population growth and urbanization has become a fundamental concern for sustainable development practitioners. The study investigates the changes in LULC within the Sundarbans, which is renowned as one of the largest mangrove forests globally (Yirsaw et al. 2017; Sun et al. 2018). Despite ongoing preservation commitments, the Sundarbans are threatened mainly by natural and human degradation (Islam and Bhuiyan 2018; Begum et al. 2022). In spite of their critical contribution to human and ecosystem welfare, mangrove forests have been declining globally at an alarming rate during the past 40 years (Worthington et al. 2020; Bunting et al. 2018). More specifically, natural disasters such as cyclones, typhoons, and land erosion have destroyed approximately 25% of the world's mangroves since 1984 (Islam et al. 2019; Bhargava et al. 2021). In addition, a significant amount of mangrove forest area is continually being transformed by human-induced activities such as deforestation for aquaculture, agriculture, and tourism industry (CEGIS 2007; Dutta et al. 2013). Therefore, the rapid changes in LULC have threatened the sustainability of land management and disrupted the socio-environmental systems in this area. Recent studies highlight the need for a thorough investigation of past, present, and future LULC changes in the Sundarbans for effective policy intervention (Ahmad et al. 2023; Islam et al. 2016a, b; Muttitanon and Tripathi 2005).

The effects of climate change and its associated factors on mangroves make them highly vulnerable (Mukherjee and Ashis 2021). These factors include sea level rise, high water events, storms, precipitation, temperature, CO₂ levels in the atmosphere, ocean circulation patterns, ecosystem health, and human responses to climate change (McKee 2004; Subramanian et al. 2023; Singh et al. 2022). The Sundarbans, recently designated as a Ramsar Site (<https://rsis.ramsar.org/ris/2370>) and a site recognized as a World Natural Heritage site by the United Nations Educational, Scientific and Cultural Organization (UNESCO), has not received much attention from researchers despite being one of the most rapidly changing regions concerning LULC (Hoque et al. 2020). Bangladesh's coastal region, including the Sundarbans, is considered one of the top fifteen high-risk areas globally. This region is exposed to environmental hazards such as cyclones, storm surges, rising sea levels, floods, shoreline erosion, land degradation, salinity intrusion, and subsidence (McGranahan et al. 2007; Roy et al. 2022; Murshed et al. 2022; Dasgupta et al. 2017). Since it is impossible to prevent these natural phenomena, it is crucial to conduct vulnerability assessments and implement effective remedial measures to mitigate their impacts.

A study by Murali et al. (2013) concluded that adaptation and mitigation are the best approaches to disaster management. Instead, the aim is to minimize their effects on humans, property, and the environment. Vulnerability assessment plays a crucial role in simplifying complex and interconnected parameters into a more manageable and understandable form, thereby serving as an effective tool for management (Nguyen et al. 2016). Recent research has explored various aspects related to the Sundarbans, such as historical LULC changes using remote sensing techniques (Abdullah et al. 2019; Hoque et al. 2019a, b), forest co-management documentation (Begum et al. 2022), mapping of mangrove erosion and progradation (Bhargava et al. 2021; Chowdhury and Hafsa 2022), mangrove recovery after natural disaster like tsunami and coastal subsidence (Prabakaran et al. 2021; Ramakrishnan et al. 2020), mapping forest degradation (Dalagnol et al. 2023), remote sensing review for mangroves (Wang et al. 2019), mangrove forest phenology analysis (Pastor-Guzman et al. 2018), hazard induced vulnerability analysis (Rehman et al. 2021) and alternative management scenarios (Roy and Gow 2015). Many studies have incorporated the coastal vulnerability index (CVI) into their assessments of mangrove vulnerability and degradation in Bangladesh's Sundarbans (Mondal et al. 2022; Mahmood et al. 2020; Hoque et al. 2019a, b). However, studies that quantitatively assessed the historical LULC changes and associated vulnerability based on different physical, socio-economic, and environmental factors are rare. This paper tried to fill this gap by applying an integrated approach considering LULC dynamics and developing a site-specific vulnerability map to address specific mitigation measures. It will be the first study that simultaneously analyze decadal LULC change detection with vulnerability assessment incorporating cutting-edge advanced geographic information systems (GIS) and remote sensing platforms. To manage the complexity of assigning suitability classes, a fuzzy expert system combined with multicriteria decision-making (MCDM) approach can effectively assess mangrove forest vulnerability. In MCDM, fuzzy set membership is used to standardize criteria (Ayu Purnamasari et al. 2019; Aydi et al. 2016), and fuzzy set theory models continuous factors for suitability assessment within GIS analysis. However, most studies have used either MCDM or fuzzy sets alone, resulting in poorly managed factor weights or incorrect suitability index calculations. Therefore, combining MCDM with fuzzy set theory can reduce subjectivity in assessments. The integrated use of GIS, fuzzy sets, and MCDM significantly improves the effectiveness and accuracy of flood vulnerability assessments (Nikolova and Zlateva 2017).

This study makes the following contributions. Firstly, it integrates multiple factors influencing LULC changes, including socioeconomic, geophysical, and climatic parameters. Secondly, it offers valuable methodological guidance

for future research aimed at efficiently tackling the spatial and spectral challenges associated with remotely acquired data when integrating LULC analysis with vulnerability assessment in a diverse landscape. Thirdly, by providing insights into vulnerable areas within the mangrove region and the drivers of LULC changes, this study directly contributes to formulating effective policy interventions for preserving the Sundarbans. These practical relevances enhance the impact of research in promoting sustainable development and environmental conservation. Despite its global significance, this region has not received as much attention from researchers as other mangrove areas, making the study particularly valuable in filling this gap. In this connection, the specific objectives are to (a) analyze the significant past and present LULC changes in the Sundarbans and (b) develop site-specific vulnerability maps based on physical, socioeconomic, and environmental factors.

The next section provides a concise overview of the study area and introduces the research framework. Section 3 describes the data and methods, while section 4 presents and discusses the results. Our conclusion and policy recommendations are discussed in section 5.

Study area and conceptual framework

Description of the study area

The Sundarbans constitute the largest mangrove forest globally, located between $21^{\circ}31'$ and $22^{\circ}30'$ north and 89° and 90° east (Hoque and Datta 2005). Four administrative units in Bangladesh monitor the Sundarbans, namely Chandpur, Sarankhola, Satkhira, and Khulna (Quader et al. 2017). Within these four ranges are five subdistricts: Sarankhola, Mongla, Dacope, Koyra, and Shalm Nagar (Fig. 1).

The Sundarbans, a vast mangrove forest spanning across India and Bangladesh, is crisscrossed by a network of numerous rivers and distributaries. These waterways serve as vital conduits, delivering essential elements to sustain the delicate balance of the ecosystem. Over time, the edge of the Sundarbans have experienced increase in anthropogenic activities due to livelihood dependence, housing material collection, fuelwood collection, and expanded shrimp farming. There has also been an increase in tourism and commercial transportation in the Sundarbans' streams (Mahmood et al. 2021).

In Bangladesh, the Sundarbans contribute significantly to the gross domestic product (GDP) through their direct and indirect benefits to livelihood (Giri et al. 2015). A significant expansion of shrimp cultivation has taken place in the Khulna, Satkhira, and Bagerhat districts of Bangladesh (Karim et al. 2019; Akber et al. 2017).

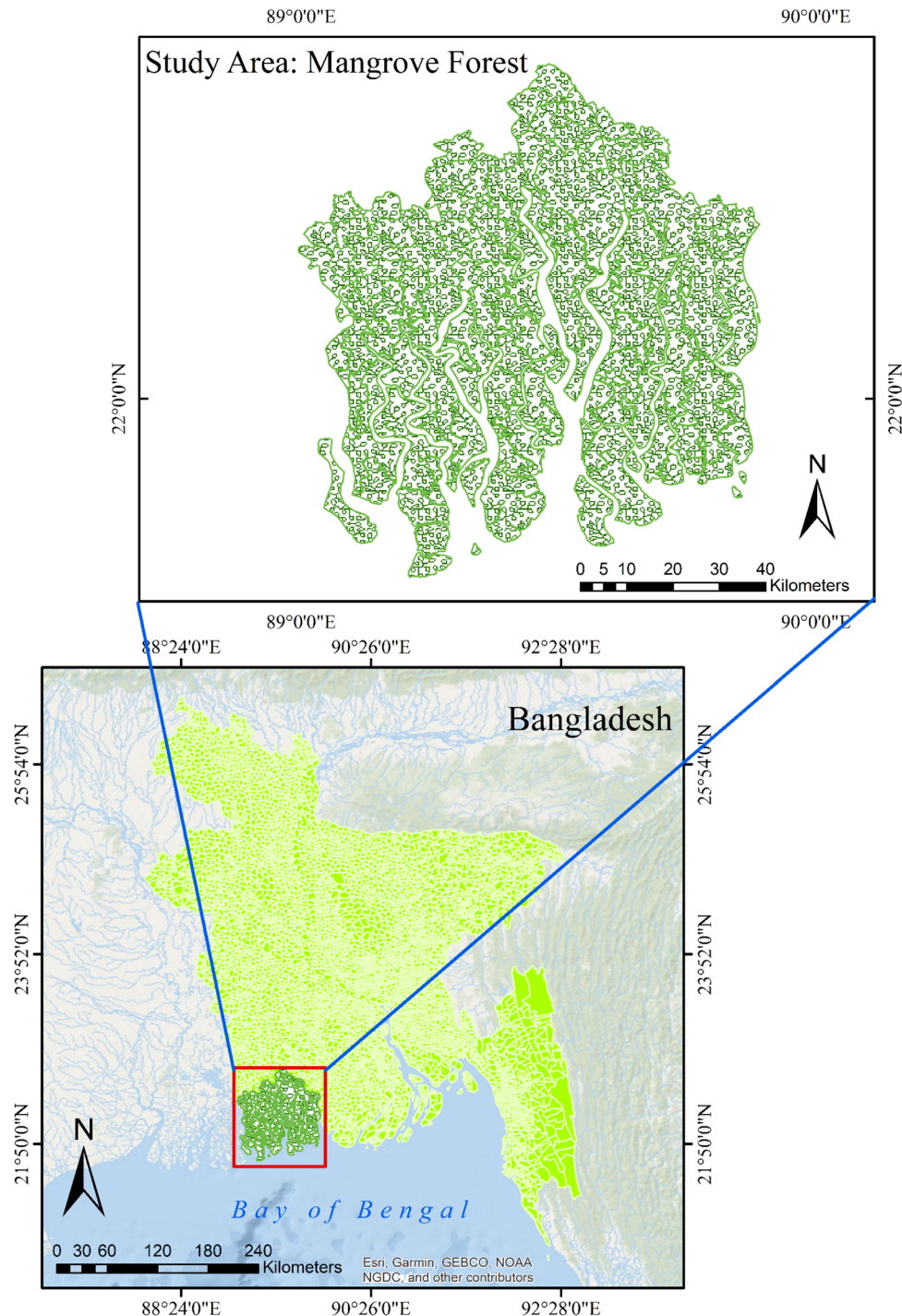
Conceptual framework for LULC change detection and vulnerability analyses

The research was carried out in two phases, as illustrated in Fig. 2. First, we examine the study area's LULC changes over 21 years (2000–2021) by creating LULC maps for five different periods, namely 2000, 2005, 2010, 2015, and 2021. As LULC classifications represent a crucial factor in evaluating mangrove vulnerability, the change detection trends are considered during the vulnerability analysis (Seyam et al. 2023; Swain et al. 2022; Islam et al., 2022). Second, we develop a final vulnerability map for mangrove areas to predict potential vulnerability scenarios. To comprehensively evaluate the vulnerability of mangrove forests to climate change, we conducted a thorough analysis encompassing socioeconomic, geophysical, and climatic factors. The vulnerability analysis employed a fuzzy expert-based MCDM approach.

We refer to previous studies to identify the underlying criteria in this study. For example, Mondal et al. (2022) investigated the vulnerability of mangrove regions along the coastal regions of West Bengal. In order to assess vulnerability, the study considered factors such as geomorphology, shoreline change rate, sea level rise, regional elevation, coastal slope, bathymetry, and mean tidal range, as well as the density of mangroves. Murshed et al. (2022) examined twenty-three factors that represented the three components of threat: environmental hazards, geo-environmental attributes, and anthropogenic modifications. In this paper, we select eight criteria focusing on topography, geology, and climate. Each criterion was used to generate a vulnerability map. Subsequently, those criteria were reclassified into different vulnerability classes, namely very low (V1), low (V2), moderate (V3), high (V4), and very high (V5) vulnerability.

The eight criteria are introduced in Fig. 2, and each criterion's rationale will be explained in the subsequent discussion. First, LULC information provides valuable insights into cultural characteristics, urbanization, agricultural practices, and the presence of native and artificial vegetation (Simon et al. 2023). Including these details in vulnerability analyses are necessary since they provide information about the overall agricultural land use in the study area. The resulting map consists of five classes: water bodies, mangrove forests, built-up areas, aquaculture sites, and other categories. Hereby, water includes all kinds of large water bodies, such as rivers, lakes, and canals. The forest includes all kinds of vegetation, so the vegetation density could differ. As the detection and classification of vegetation density is unimportant, we combined all vegetation types into one class. Built-up comprises all kinds of man-made infrastructure such as buildings, factories, roads, ports, markets, etc. Fisheries and salt farms are examples of aquaculture, whereas mudflats,

Fig. 1 Map showing the location of the study area. Source: Authors' development using ArcGIS 10.8.2® software



coastal flats, exposed soils in riverine areas, wetlands, coastal marshes, and newly accreted lands are examples of other categories. Second, population density within a specific area positively correlates with a higher likelihood of mangrove deforestation. For instance, human activities such as settlement development and transportation infrastructure contribute to the degradation of coastal ecosystems and biodiversity loss (Murshed et al. 2022; Roy et al. 2017). Deforestation significantly reduces the

protective function of mangroves against environmental hazards, thus amplifying vulnerability.

The third factor is the elevation of a specific location relative to the average sea level. As a result, it is crucial to assess vulnerability and identify areas susceptible to sea-level increase (Roy et al. 2022). In coastal areas of low elevation, vulnerability is high, while in coastal areas of higher elevation, vulnerability is low. Fourth, coastal hazards are more likely to occur

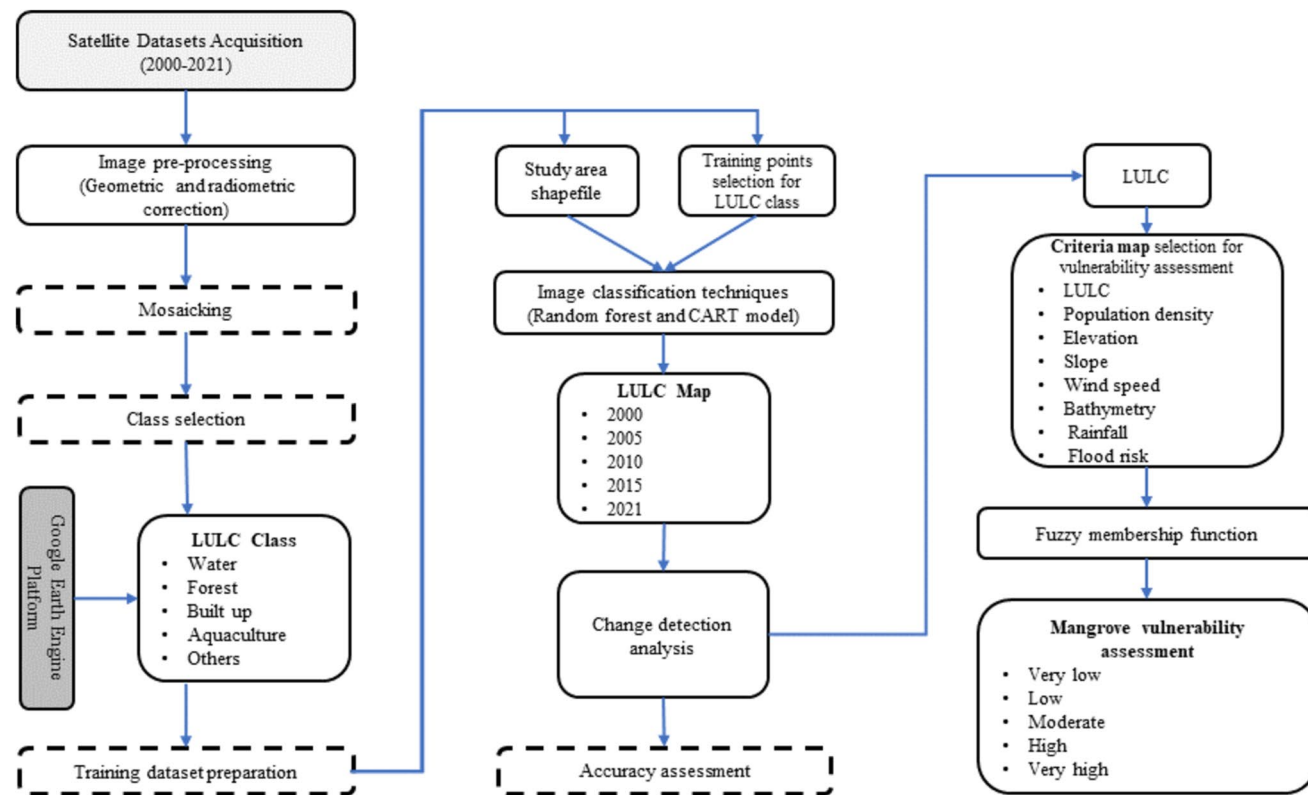


Fig. 2 Methodological framework for LULC change detection and vulnerability assessment of mangrove forest. Source: Authors' own illustration

in gradual, steep slope areas (Islam et al. 2015). Fifth, strong winds along the ocean coast can enhance astronomical tides, leading to wave overtopping and subsequent coastal flooding. The speed and direction of the wind also affect the location and type of wave breaks, which can result in shoreline erosion (Murshed et al. 2022). The sixth principle is that bathymetry denotes water depth measurement, which is essential for wave analysis, hydrodynamic modeling, and inundation studies (Islam et al. 2016a, b). We establish five bathymetry depth categories, assuming that areas with greater depth would be less vulnerable than those with shallow depths. Shallow water has a higher potential for extensive penetration and increased vulnerability. Seventh, intense rainfall can lead to pluvial floods and potentially induce erosion in coastal regions. Relatedly, coastal areas experience various types of floods, including monsoon or fluvial floods, flash floods, and tidal floods. Tidal floods are widespread in coastal zones, where high tides regularly submerge extensive areas. Strong southern winds and runoff from major rivers cause the Bay of Bengal's sea surface to rise during intense monsoon storms (PDO-ICZMP, 2004). Finally, flood events have immediate disastrous impacts on human lives and the environment. Furthermore, the erosive force of the water can gradually undermine the foundation materials of infrastructure, leading to eventual collapse (Alam et al. 2021).

Data and methods

Data sources

The following two subsections provide details on data sources and information used for the LULC change detection approach and vulnerability analysis.

Data for LULC change detection analysis

For LULC change detection analysis, we use the Google Earth Engine (GEE) platform to extract data on land use (Habib and Connolly 2023). More specifically, we use two different data sources. First, we apply the top-of-atmosphere (TOA) reflectance data from LANDSAT Collection 2 Tier 1. This dataset encompassed six different bands, each offering a spatial resolution of 30 m. To ensure the robustness of the training process, we meticulously selected imagery with minimal cloud cover, typically amounting to less than 5%.

Additionally, the study employed the calibrated TOA reflectance data from LANDSAT 8 Collection 2 Tier 1 for the 2015 and 2022 datasets. Like the LANDSAT 7 dataset, this entailed seven distinct bands with a comparable 30-m

Table 1 Types and sources of data used for the study

SL No.	Data	Description	Source
i.	LULC	Developed from Landsat 9 images in the GEE Platform	USGS (2021)
ii.	Population density	Population density per pixel at 100-m resolution	WorldPop (2015)
iii.	Elevation	Accumulated from SRTM (30-m resolution)	SRTM (2023)
iv.	Slope	Accumulated from SRTM (30-m resolution)	SRTM (2023)
v.	Wind speed	Mean wind speed (250-m horizontal grid spacing)	Global Wind Atlas (2022)
vi.	Bathymetry	Data initially at a 15 arc-second resolution has been resampled to 900 m.	Global Wind Atlas (2022)
vii.	Rainfall	Average precipitation data (1990–2020)	CHRS (2020)
viii.	Flood risk	Flood risk map developed by BARC	HDX (2021)

USGS=United States Geological Survey; CHRS=Center for Hydrometeorology and Remote Sensing; BARC=Bangladesh Agricultural Research Council; HDX=Humanitarian Data Exchange

resolution. We took utmost care in selecting imagery with the lowest possible cloud cover to maintain data integrity and optimize model performance. The careful selection of satellite imagery from these two sources allowed us to capture temporal variations and changes in the study area over the specified time frame. By ensuring consistent data quality, including calibrated TOA reflectance, and mitigating cloud cover interference, our analysis was intended to be more accurate and reliable.

Data for vulnerability analysis

Data from satellite images, including Landsat, GEE, and Shuttle Radar Topography Mission (SRTM) Digital Elevation Models (DEMs), hydrological data, and climatic features, were used to assess vulnerabilities in the Sundarbans mangrove regions. Table 1 summarizes several primary datasets, along with their sources and specifications.

Methods

In the following method section, we introduce the two-step approach, first identifying historical LULC changes and second implementing the vulnerability analysis.

LULC change detection analysis

In this study, we use the random forest (RF) model, a prominent ensemble learning technique widely applied in machine learning, to effectively address the classification and regression tasks. RFs are renowned for their proficiency in enhancing prediction accuracy by amalgamating multiple decision trees. The construction of the RF model followed a systematic step-by-step process, as shown in Fig. 3.

Initially, we created an ensemble of decision trees, with each tree being independently trained on a randomly selected subset of the data. This sampling approach, also called the

bagging procedure, adhered to an 80–20 ratio, partitioning the data into training and testing subsets (Billah et al. 2023). Data sampling utilized pixel-based and visual satellite image-based analyses, ensuring a comprehensive and diverse representation of the study area.

Upon the completion of individual decision tree training, the predictions from each tree were aggregated to derive the outcome, which is the LULC change map. In the context of classification tasks, the most frequently predicted class among the ensemble of trees was selected as the ultimate classification result. The aggregated predictions were averaged for regression tasks to generate the final continuous values. Adopting the RF model, complemented by the bagging procedure and meticulous data sampling through pixel-based and visual satellite image-based analyses, fortified the efficacy and robustness of our approach. This enabled a reliable analysis of the classification and regression tasks, fostering a deeper understanding of the land use dynamics in the study region and laying the groundwork for informed decision-making and further research pursuits.

We adopted a meticulous approach to selecting data points in each annual assessment, primarily relying on pixel-based evaluations. However, when encountering challenging situations in pixel-based training, we resorted to visual satellite-based image analysis and point selection methods. As a result, the number of training points varied for each year. This adaptive strategy offers distinct advantages over conventional model training processes, enabling us to achieve heightened accuracy in detecting land use changes.

Given the dynamic nature of land use over time, employing consistent pixel-based training across all years may yield suboptimal results. To address this, we implemented the following approach. First, we identified specific pixels and assigned them to land use categories 2000. Second, we tracked the same pixels from 2005 to 2021 to monitor any alterations in their land use classification. If a particular pixel changed, such as transitioning from a forest to a

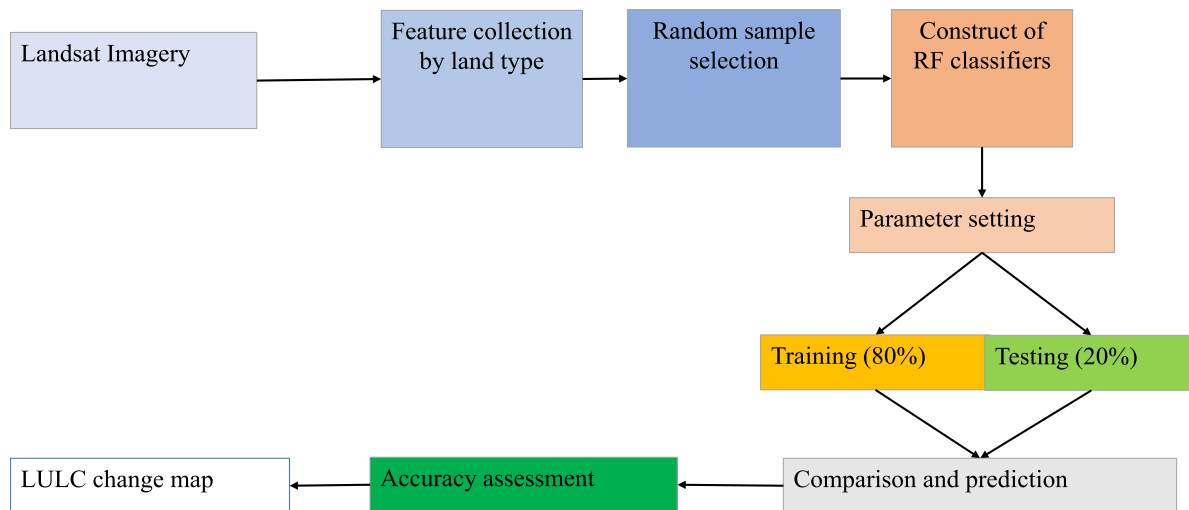


Fig. 3 The process of applying the random forest model. Source: Authors' own illustration

built-up area during these years, we appropriately modified the land use classification. This iterative process was carried out for all subsequent years, ensuring a more accurate depiction of evolving land use patterns.¹

Upon acquiring the land use data as .tiff files from GEE, we proceeded with data extraction and analysis using ArcGIS Pro. In tandem, we evaluated land use change for each year and the cumulative change over the entire study period. To gauge the accuracy of our data set, we employed confusion matrix measurement. As a result, the predictive performance of the RF models could be comprehensively assessed. This confusion matrix measurement can be specified as follows:

$$\text{Accuracy} = \frac{TP + TN}{TP + TN + FP + FN} \times 100\% \quad (1)$$

where TP , TN , FP , and FN are used to indicate the correct identification of true positive, true negative, false positive, and false negative for pixels, respectively. The numerator of this fraction defines the correct prediction, whereas the denominator refers to the total cases. Furthermore, we sought to corroborate our results by incorporating the Classification and Regression Tree (CART) model. This parallel approach ensured a robust validation of our findings and allowed for a more precise estimation of nonparametric nonlinear trends, a capability beyond the scope of the RF model. Notably, the CART model employed the same data points as the RF model for each year, ensuring consistency in the analytical process (Appendices 1–6).

The data processing in ArcGIS Pro involved the initial import of the .tiff image file obtained from GEE. Subsequently, we utilized the 'extract by mask tool' to extract pertinent information based on the land classification assigned in GEE. By aggregating the number of pixels for each land classification, we accurately calculated the corresponding area of each pixel. Subsequently, we converted these values into the standardized unit of square kilometer (Sq. km).

Vulnerability analysis

In the second stage, we created a vulnerability map, employed a multicriteria approach, including the eight criteria described in the conceptual framework, and utilized fuzzy membership functions (FMF) for reclassification, as shown in Fig. 4.

We implemented FMF within the ArcGIS 10.8.2 environment for each criterion. These membership functions were chosen based on their best-fit values ranging from 0 to 1. A literature review and reference to previous studies (e.g., Murshed et al. 2022; Han et al. 2022) led to the selection of four FMFs.

We used linear, small, MS large, and Gaussian FMF to standardize the selected criteria (Equations (2)–(5)).

$$\mu(x) = \begin{cases} 0 & x \leq a \\ \frac{x-a}{b-a} & a < x < b \\ 1 & x \geq b \end{cases} \quad (2)$$

$$\mu(x) = \frac{1}{1 + \left(\frac{x}{f2}\right)^{f1}} \quad (3)$$

¹ Because of this approach, the data points associated with each land use category were ascertained. The number of data points varied yearly due to the dynamic nature of land use, which changes over time. Appendix E shows the number of data points by land use category: water, forest, built-up, aquaculture, and others.

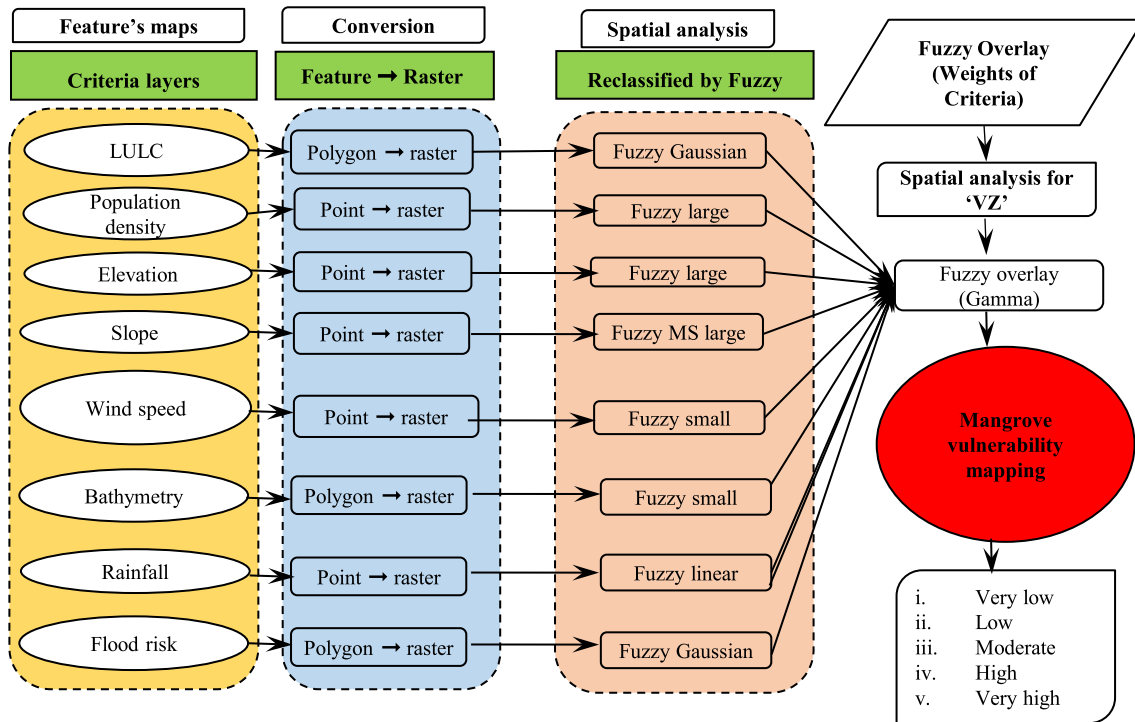


Fig. 4 Steps followed for mangrove vulnerability assessment. Source: Own illustration

$$\mu(x) = \frac{1}{1 + \left(\frac{x}{f^2}\right)^{-f^1}} \quad (4)$$

$$\mu(x) = e^{-(f^1 \times (x - f^2)^2)} \quad (5)$$

Equation (2) represents the x coordinate values, where a and b denote the crisp values². For the fuzzy small and fuzzy MS large membership functions, respectively, f^1 and f^2 denote the spread and midpoint, while x denotes the crisp value. Each criterion has a different value for f^1 and f^2 . The FMF, which includes fuzzy large, fuzzy MS large, fuzzy small, fuzzy Gaussian, and fuzzy linear, was applied within the ArcGIS 10.8.2 environment Table 2.

Next, Fig. 5 shows the vulnerability maps for each criterion using five distinct vulnerability classes ranging between a lower level of vulnerability (V1) to a high level of vulnerability (V5). A rise in population density within a particular region correlates with an increased probability of mangrove deforestation. Greater population density indicates greater vulnerability, while lower density signifies a lower level of vulnerability. Mangrove regions characterized by

Table 2 Vulnerability of mangroves with fuzzy membership function (FMF)

SL. No.	Features	FMF		Types of FMF
		Midpoint	Spread	
i.	LULC	2	0.1	Gaussian
ii.	Population density	5	0.473	Large
iii.	Elevation	28.5	5	Large
iv.	Slope	20.39	5	MS Large
v.	Wind speed	4.929	5	Small
vi.	Bathymetry	-6	5	Small
vii.	Flood risk	4	0.1	Gaussian
		Minimum	Maximum	
viii.	Rainfall	45.74	133.15	Fuzzy Linear

Source: Authors' own compilation

lower elevations are classified as having high vulnerability, whereas those with higher elevations are identified as having lower vulnerability. Similarly, areas of mangroves featuring gradual slopes are more vulnerable to coastal dangers compared to regions with steeper slopes. On the other hand, the potential impact of extreme occurrences involving exceptionally high water levels and wind speeds on mangrove regions. Consequently, a greater wind speed within a specific location increased the likelihood of vulnerability in mangroves, while

² The fuzzy set assigns a value ranging from 0 to 1, encompassing both 0 and 1. In contrast, the crisp set assigns the value strictly as either 0 or 1.

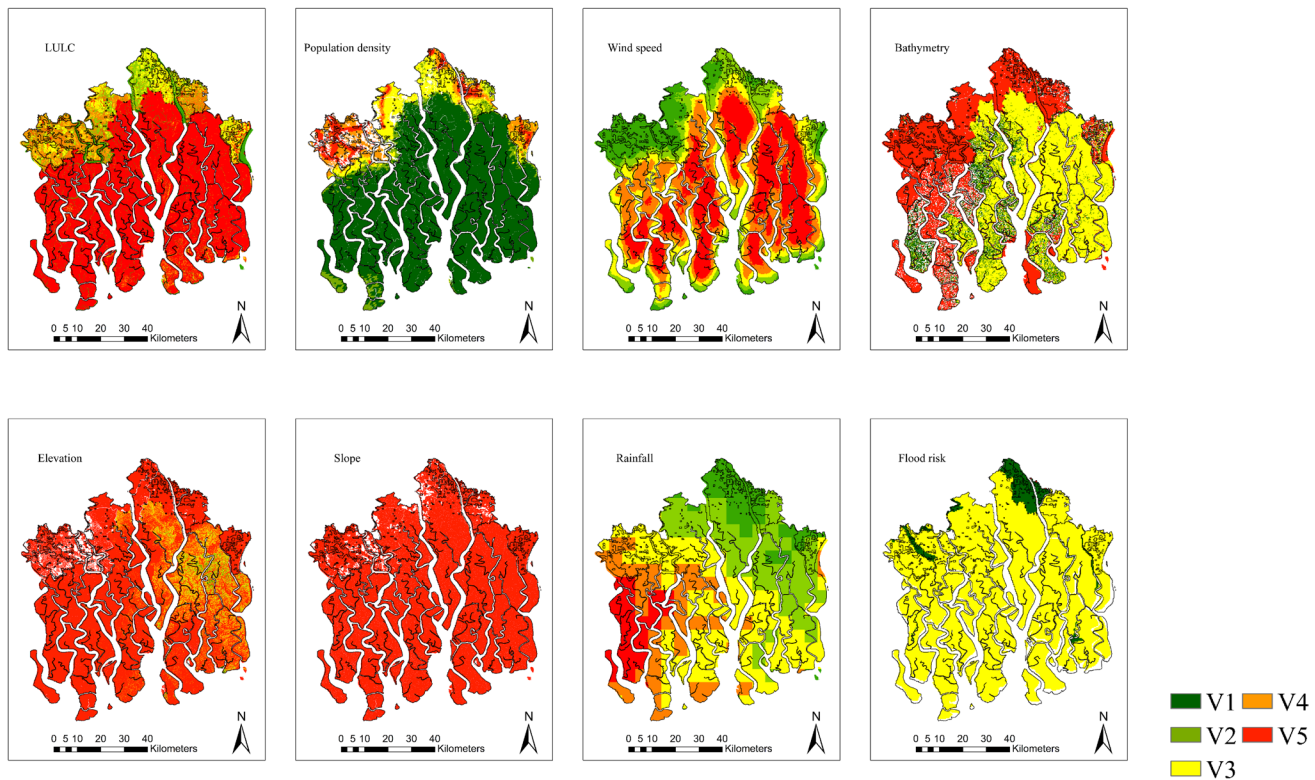


Fig. 5 Reclassified mangrove vulnerability map of different criteria layers used in this study. Note: very low (V1), low (V2), moderate (V3), high (V4), and very highly (V5) vulnerable areas. Source: Authors' own calculations

lower wind speeds were associated with lower vulnerability. Moreover, concerning the bathymetry index, areas with greater water depth were deemed less vulnerable compared to shallower regions. However, study shows that higher levels of rainfall could lead to erosion within the mangrove forest, ultimately resulting in diminished productivity and growth, as identified by Sahoo and Bhaskaran in 2018. Hence, the study acknowledged that regions experiencing higher annual precipitation were more prone to mangrove vulnerability. Furthermore, the study acknowledged the prevalence of tidal floods in coastal areas, categorizing regions affected by such floods as highly vulnerable while those susceptible to monsoon floods are considered less vulnerable. Lastly, the research factored in the vulnerability of existing mangrove areas as high, compared to river and water body zones, which were deemed lower vulnerability.

Finally, the eight vulnerability maps for each criterion need to be overlaid to understand the whole extent of vulnerability. For this purpose, we employ fuzzy overlay tools that facilitate the examination of phenomena that could pertain to several sets within a multicriteria overlay approach. However, fuzzy overlays examine the relationships among these sets' members and determine the phenomenon's potential presence within each set. We apply a fuzzy gamma overlay, employing the expression provided by ESRI (2016):

$$\mu(x) = (\text{FuzzySum})^y \times (\text{FuzzyProduct})^{1-y} \quad (6)$$

In order to generalize the fuzzy gamma overlay function, a gamma value of 0.9 was applied (ESRI 2016). Based on Jenks Natural Breaks algorithm (Jenks 1967), the vulnerability map was reclassified into five categories. According to Jenks and Caspall (1971), this categorization procedure organized the information according to inherent patterns found within the database.

Results and discussions

Following our two-step approach, we present the LULC changes identified over the 21-year period and the results of the vulnerability assessment.

LULC changes in the Sundarbans

Figure 6 visually represents the LULC changes in the Sundarbans region from 2000 to 2021. In each sub-figure, the blue color signifies water bodies, encompassing rivers, lakes, and canals, while the green area represents the forest and vegetation. Conversely, the red, orange, and pink areas correspond to different built-up structures, aquacultural farms, and other

land uses, respectively. One can note the substantial reduction in forest area, particularly in the northern part of the Sundarbans, which has been replaced by various human activities, including buildings, roads, and infrastructures, as well as shrimp farms, which is completely aligned with other studies (Hossain et al. 2022; Karim et al. 2019; Akber et al. 2017; Faruque et al. 2022; Halder et al. 2020; Khan et al. 2021).

One plausible reason behind this deforestation could be attributed to the population increase in the Sundarbans regions, leading to escalated demands for natural resources. Additionally, the local inhabitants' continuous exploitation of these resources may have contributed to the diminishing forest cover (Dutta et al. 2013; Béland et al. 2006). Moreover, inadequate governmental regulation and contradictory policies concerning preserving the mangrove forest could contribute to the observed deforestation (Ishtiaque and Chhetri 2016). The absence of coherent policies may have led to ineffective conservation measures and allowed for unchecked expansion of human-induced activities into forested areas.

To obtain a better understanding of these changes, we compiled the area of each land class for different years. Figure 7 that illustrates a substantial and continuous decrease in forest land over the observed period. At the same time, there has been a notable increase in built-up areas and aquaculture. Water bodies and other land classes exhibit mixed trends, with fluctuations in their respective extents over time. One can note a persistent decline in forest cover. Notably, the most significant percentage change in the forest area occurred between 2000 and 2005, amounting to approximately 5.5%. However, this rate of change moderated during the subsequent period from 2010 to 2015 (−1.45%). Conversely, aquaculture and built-up areas have steadily increased over the periods. Additionally, Appendix F provides the area changed values, denoting the total land area that transformed within specific time frames. The rate of change, calculated as the average area change per year, reveals that each year, the forest area has been altered by approximately 20 to 65 sq. km. In contrast, aquaculture has increased to 17 to 32 sq. km per year. Overall, the water bodies and forest area have decreased by 0.04% and 14.4%, respectively. On the other hand, urban areas, shrimp farms, and other areas have increased, ranging between 2.2 and 8.4%.³

Finally, Fig. 8 spatially illustrates the observed LULC changes over the total time horizon from 2000 to 2021. The unchanged forest areas are presented in green, while the yellow pixels signify the conversion of forest land into

other land classes, such as dunes and sand beaches. Land use changes and forest land conversion are concentrated within the northern region of the Sundarbans. Notably, the forest area has transformed into built-up structures, depicted in red, and aquaculture, depicted in orange.

Our findings regarding LULC changes align with the research conducted by Abdullah et al. (2019) related to coastal areas of Bangladesh. Over the last 28 years, from 1990 to 2017, the study noted an overall growth in agricultural land (5.44%), built-up areas (4.91%), and river areas (4.52%). Another investigation conducted by Chowdhury and Hafsa (2022) also explored the conversion of numerous non-vegetated regions outside the Sundarbans mangrove forest in Bangladesh into water bodies as a result of shrimp farming. Additionally, a LULC analysis study by Faruque et al. (2022) revealed a remarkable increase in aquaculture and a significant decrease in agriculture in mangrove forest areas of Bangladesh. These works have collectively corroborated the significant transformation of land use and the conversion of forest areas into various alternative land classes.

To validate our LULC results, we tested the accuracy of the RF and CART models and subsequently compared their results. Appendix 7 shows that the RF model demonstrated accuracy levels ranging from 70 to 86%, whereas the CART model exhibited an accuracy close to 100% (Table 7). These outcomes indicate that both models are sufficiently accurate in their predictions.

The accuracy of the RF model can be contrasted with findings from Billah et al. (2023). They discovered that when conducting land cover mapping to evaluate rapid flood damage in the northeastern region of Bangladesh using Sentinel-1 & 2, the RF classifier yielded superior results of 90% accuracy level as opposed to the maximum likelihood classification that demonstrates an accuracy level of 74%. Conversely, Mondal et al. (2019) found that the RF-generated classified image achieved an overall accuracy of 93.44%, whereas the CART-generated image achieved 92.18% for mapping mangroves in West Africa. The consistent results from both models strongly indicate a progressive decline in the Sundarbans mangrove forest over time.

Vulnerability assessment of the Sundarbans

The right panel of Fig. 9 shows that approximately 4% (135 km²) of the coastal area fell within the very low vulnerability class, while 36% (1311 km²) was classified as highly vulnerable. Furthermore, the left panel of Fig. 9 visualizes the spatial distribution of the different vulnerability classes. It can be seen that 19% (714 km²) and 27% (987 km²) of the region were categorized as low and moderate vulnerability areas, respectively. Furthermore, 14% of the area (529 km²)

³ For a detailed description LULC changes in area changes see Appendix F.

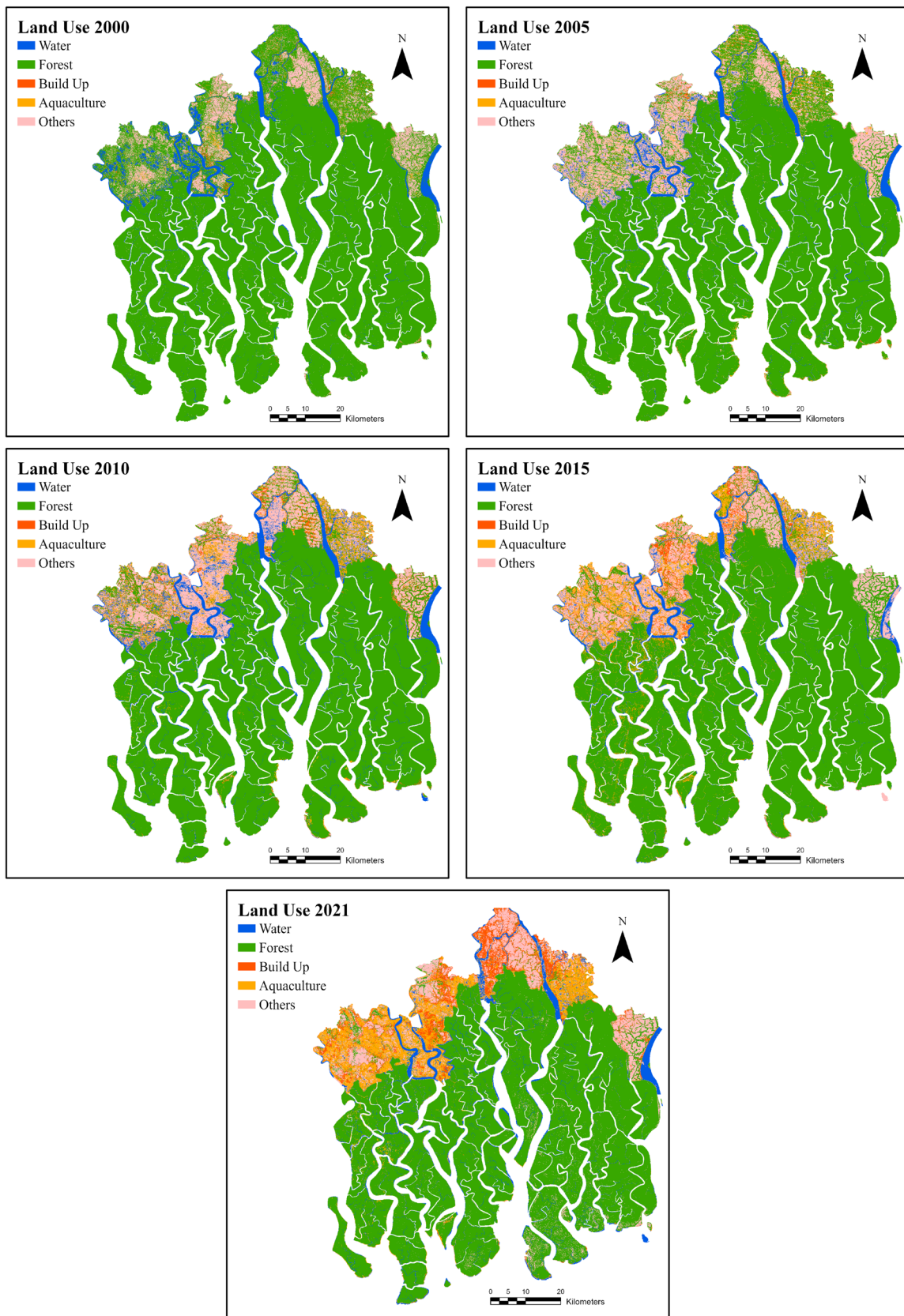


Fig. 6 Visualization of LULC of Sundarbans from 2000 to 2021 Source: Authors' own preparation

Fig. 7 Percentage of LULC changes over time between 2000 and 2021. Source: Authors' own compilation

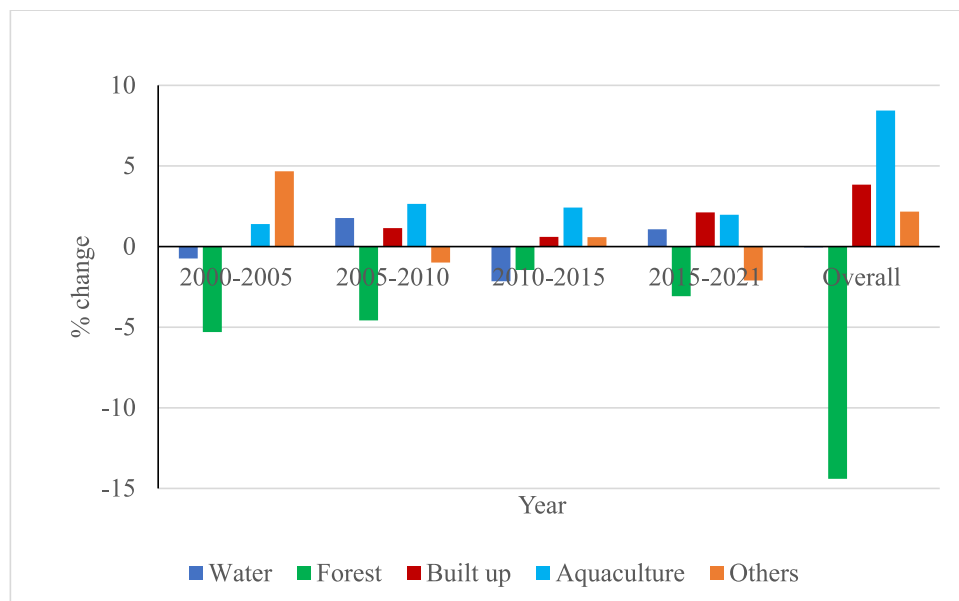
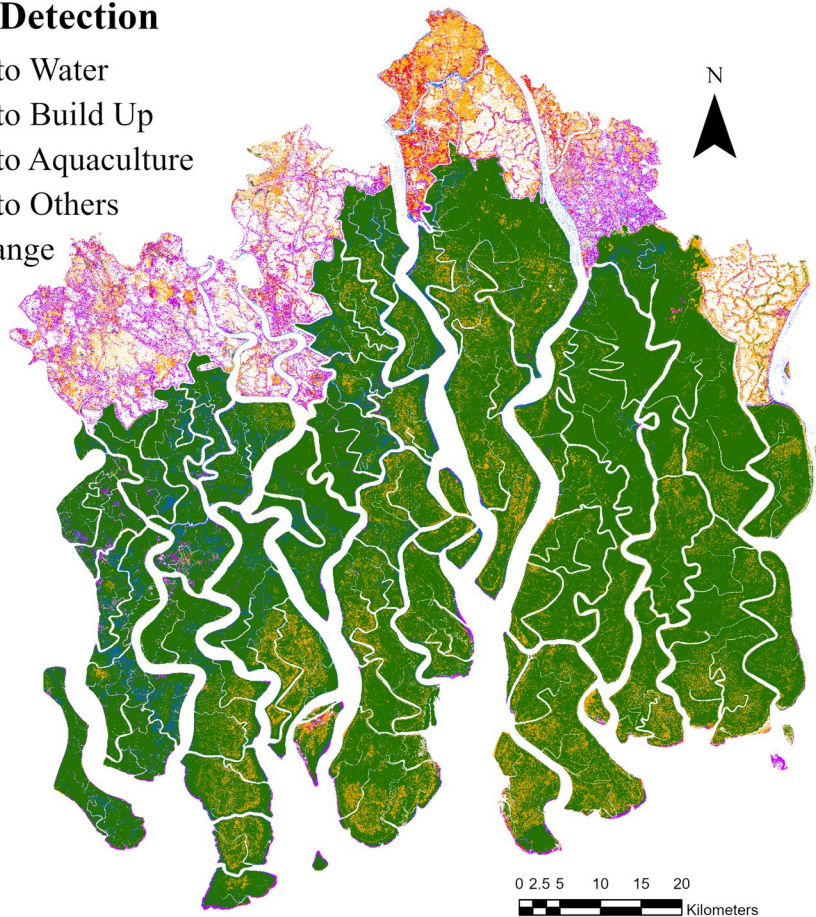


Fig. 8 LULC change detection from random forest model over time (2000 to 2021). Source: Authors' own compilation

Change Detection

- Forest to Water
- Forest to Build Up
- Forest to Aquaculture
- Forest to Others
- No Change

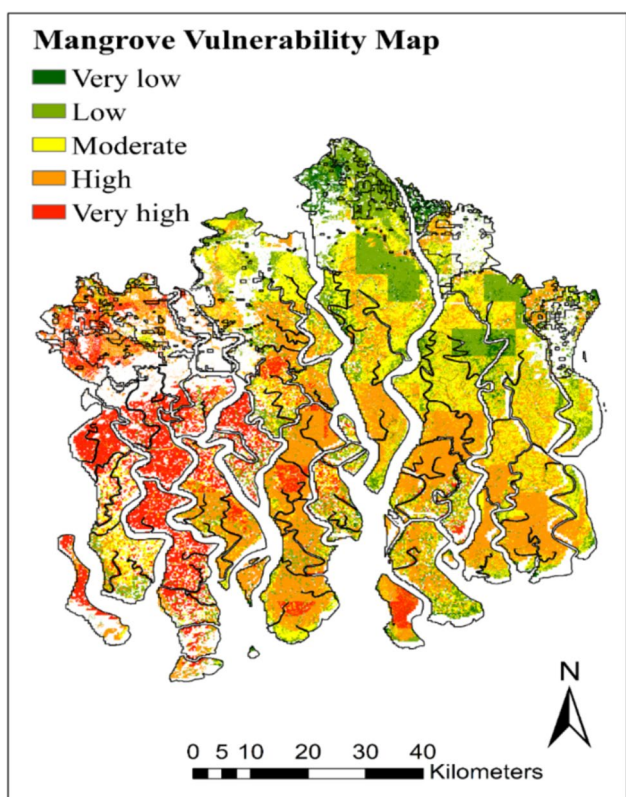


was identified as a zone with a high vulnerability for future impacts. Detailed findings of mangrove vulnerability can be found in Table 3; Fig. 9.

According to the mangrove vulnerability assessment depicted in Fig. 9, two prospective areas were identified for the implementation of afforestation and restoration

Table 3 Classified result of mangrove vulnerability

Vulnerability category	No. of pixel	Area (sq. km)	Percentage
Very low	150,254	135.23	3.68
Low	793,264	713.94	19.42
Moderate	1,097,199	987.48	26.86
High	1,456,798	1311.12	35.66
Very high	587,939	529.15	14.40

**Fig. 9** Sundarbans mangrove vulnerability map using fuzzy overlay. Source: Authors' own compilation

strategies. Areas categorized as having very low and low vulnerability were deemed stable and apt for afforestation endeavors. Consequently, regions with high vulnerability levels must be prioritized for restoration policies. Urgent restoration initiatives should be undertaken to protect these regions with high vulnerability intensity.

Conclusions and policy implications

The objective of this study was to analyze LULC changes in the coastal mangrove region of Bangladesh over the last two decades between 2000 and 2021. Additionally,

the study aimed to identify vulnerable areas within the mangrove region using a set of influential parameters. The analysis was conducted using the GEE platform and processed in the ArcGIS® environment. Based on the LULC maps from 2000 to 2021, it was observed that water bodies, built-up areas, aquaculture, and barren lands have changed by around 0.04%, 3.84%, 8.4%, and 2.2%, respectively. On the other hand, forest area has been reduced by 14.4% over the years. The highest amount, more than 5% of the forest area, decreased between 2000 and 2005. The decline in forest areas can be primarily attributed to its conversion into urban and industrial settlements, as well as the expansion of shrimp farms. These human-induced activities pose severe threats to the region's biodiversity, climate regulation, and the livelihoods of local communities dependent on the forest resources. Therefore, understanding these LULC changes is crucial for identifying the drivers of change, such as urbanization, industrial expansion, and shrimp farming. This information can guide policymakers in designing policies and strategies to address these drivers sustainably, such as implementing land-use planning regulations and promoting sustainable aquaculture practices.

In forecasting the Sundarbans' vulnerability to factors associated with LULC, population density, elevation, slope, wind speed, bathymetry, rainfall, and flood risks, the MCDM approach and fuzzy logic were employed. The analysis revealed that the highly vulnerable area accounted for 35.66% of the study area. Additionally, it showed that the moderately vulnerable area covered 26.86% of the study area, and the low vulnerable area comprised 19.42%. Policymakers can use this information to prioritize conservation efforts by promoting reforestation and afforestation programs and supporting alternative livelihood options for local communities. Furthermore, the LULC analysis conducted with the GEE demonstrated significant precision in interpreting alterations nationally, particularly within the Ganges Brahmaputra (GBM) corridor and deltaic evolution. Finally, an MCDM approach and a fuzzy expert system for forecasting vulnerability provide a predictive tool for researchers and policymakers. This prediction model can be refined and integrated into decision-making processes to anticipate future changes and proactively implement mangrove conservation measures effectively and efficiently.

The findings of this study have several limitations that affect their applicability. The MCDM and fuzzy expert systems are based on specific assumptions and criteria, which may not fully capture the complexity of real-world scenarios, potentially introducing biases and uncertainties. The study covers the period from 2000 to 2021, providing a two-decade overview but possibly missing longer-term trends or seasonal variations that could influence LULC changes and vulnerability assessments.

The spatial resolution of the analysis might be too low to capture localized variations in LULC changes and vulnerability, with finer-scale analyses potentially revealing more detailed patterns and insights. Additionally, while the study identifies urbanization, industrial expansion, and shrimp farming as major drivers, it may not fully account for other human activities, such as illegal logging, that also contribute to LULC changes. Future

research should evaluate the effectiveness of existing land-use planning regulations and conservation policies to identify gaps and develop more effective strategies. Additionally, future studies could create dynamic models to simulate future LULC changes and vulnerability under different scenarios, incorporating factors such as policy interventions, economic developments, and climate change projections.

Appendix 1

Fig. 10 Results obtained from the CART model

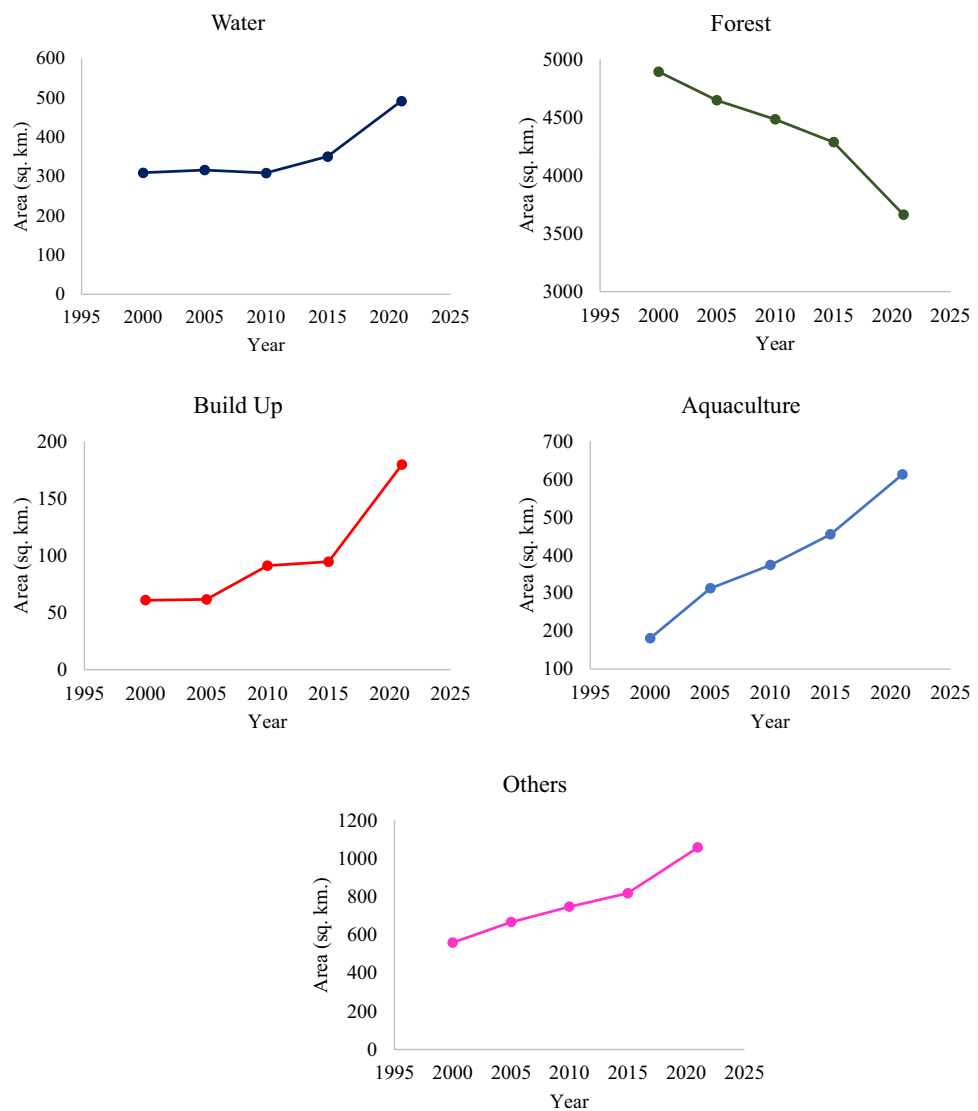


Fig 10

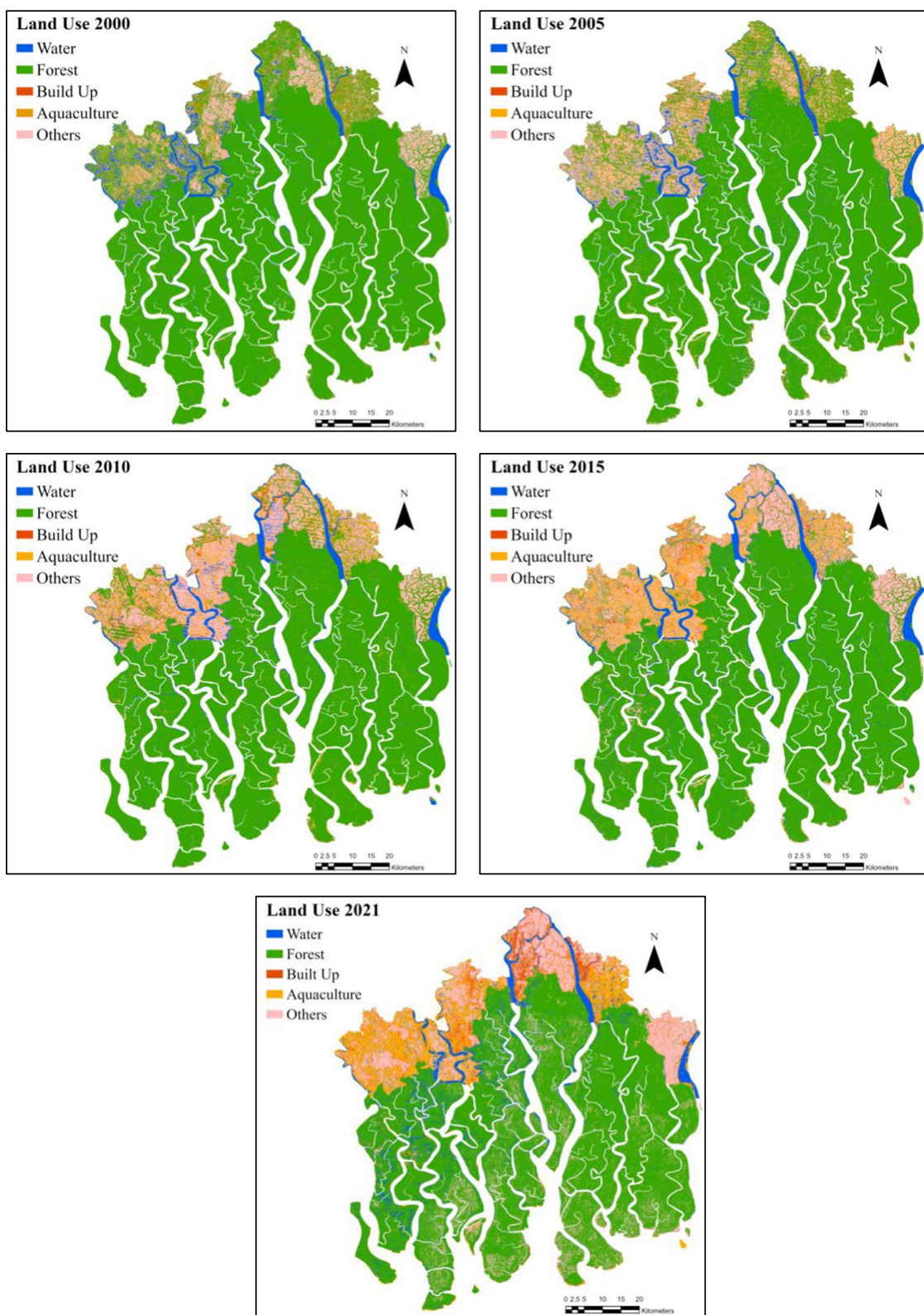


Fig. 11 LULC of Sundarbans classified using the CART model

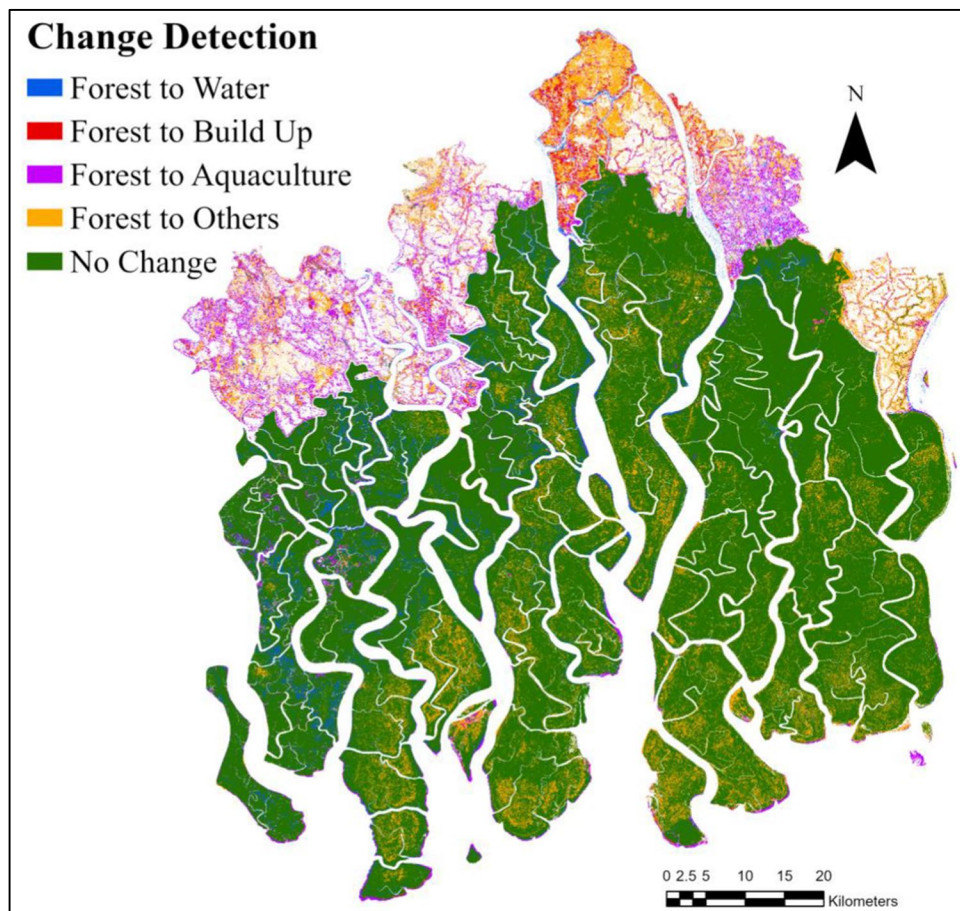
Appendix 2

Fig 11

Table 4 Percentage of LULC change by year calculated using the CART model

Year	Parameter	LULC classes				
		Water	Forest	Built up	Aquaculture	Others
2000–2005	Percentage change	0.113	−4.106	0.011	2.191	1.792
	Area changed (sq. km)	6.810	−246.523	0.640	131.512	107.561
	Rate of change (sq. km per year)	1.362	−49.305	0.128	26.302	21.512
2005–2010	Percentage change	−0.124	−2.731	0.493	1.021	1.341
	Area changed (sq. km)	−7.473	−163.931	29.579	61.310	80.516
	Rate of change (sq. km per year)	−1.495	−32.786	5.916	12.262	16.103
2010–2015	Percentage change	0.696	−3.271	0.058	1.345	1.173
	Area changed (sq. km)	41.781	−196.370	3.479	80.717	70.394
	Rate of change (sq. km per year)	8.356	−39.274	0.696	16.143	14.079
2015–2021	Percentage change	2.349	−10.389	1.417	2.633	3.990
	Area changed (sq. km)	141.031	−623.714	85.061	158.094	239.528
	Rate of change (sq. km per year)	23.505	−103.952	14.177	26.349	39.921
Overall	Percentage change	3.034	−20.497	1.978	7.190	8.295

Fig. 12 Visual change detection using the CART model



Appendix 3

Table 5 Number of land use land cover training data points by years

LULC classes	2000	2005	2010	2015	2021
Water	117	109	87	87	84
Forest	401	266	116	116	303
Built-up	55	34	27	27	223
Aquaculture	50	50	50	50	140
Others	138	106	106	106	179

Table 4

Table 6 Percentage of LULC change by year calculated using the RF model

Year	Parameter	LULC classes				
		Water	Forest	Built up	Aquaculture	Others
2000–2005	Percentage change	0.113	−4.106	0.011	2.191	1.792
	Area changed (sq. km)	6.810	−246.523	0.640	131.512	107.561
	Rate of change (sq. km per year)	1.362	−49.305	0.128	26.302	21.512
2005–2010	Percentage change	−0.124	−2.731	0.493	1.021	1.341
	Area changed (sq. km)	−7.473	−163.931	29.579	61.310	80.516
	Rate of change (sq. km per year)	−1.495	−32.786	5.916	12.262	16.103
2010–2015	Percentage change	0.696	−3.271	0.058	1.345	1.173
	Area changed (sq. km)	41.781	−196.370	3.479	80.717	70.394
	Rate of change (sq. km per year)	8.356	−39.274	0.696	16.143	14.079
2015–2021	Percentage change	2.349	−10.389	1.417	2.633	3.990
	Area changed (sq. km)	141.031	−623.714	85.061	158.094	239.528
	Rate of change (sq. km per year)	23.505	−103.952	14.177	26.349	39.921
Overall	Percentage change	3.034	−20.497	1.978	7.190	8.295

Source: Authors' own compilation

Table 7 Accuracy measurement of random forest and CART models by year

Year	Random Forest Model	CART Model
2000	0.756	~1.000
2005	0.859	
2010	0.727	
2015	0.703	
2021	0.857	

Source: Authors' own compilation

Appendix 4

Fig 12

Appendix 5

Table 5

Appendix 6

Table 6

Appendix 7

Table 7

Funding Open access funding provided by CSIRO Library Services. This research received no external funding.

Data Availability The data presented in this manuscript are available on request from the corresponding author.

Declarations

Conflict of interest The authors declare that they have no conflict of interest.

Open Access This article is licensed under a Creative Commons Attribution 4.0 International License, which permits use, sharing, adaptation, distribution and reproduction in any medium or format, as long as you give appropriate credit to the original author(s) and the source, provide a link to the Creative Commons licence, and indicate if changes were made. The images or other third party material in this article are included in the article's Creative Commons licence, unless indicated otherwise in a credit line to the material. If material is not included in the article's Creative Commons licence and your intended use is not permitted by statutory regulation or exceeds the permitted use, you will need to obtain permission directly from the copyright holder. To view a copy of this licence, visit <http://creativecommons.org/licenses/by/4.0/>.

References

- Abdullah AYM, Masrur A, Adnan MSG, Baky MAA, Hassan QK, Dewan A (2019) Spatio-temporal patterns of Land Use/Land Cover Change in the heterogeneous Coastal Region of Bangladesh between 1990 and 2017. *Remote Sens* 11(7):790. <https://doi.org/10.3390/rs11070790>
- Ahmad H, Abdallah M, Jose F, Elzain HE, Simul Bhuyan Md, Shoemaker DJ, Selvam S (2023) Evaluation and mapping of predicted future land use changes using hybrid models in a coastal area. *Ecological Informatics* 78:102324–102324. <https://doi.org/10.1016/j.ecoinf.2023.102324>
- Akber M, Islam M, Ahmed M et al (2017) Changes in shrimp farming in southwest coastal Bangladesh. *Aquacult Int* 25:1883–1899. <https://doi.org/10.1007/s10499-017-0159-5>
- Alam A, Ahmed B, Sammonds P (2021) Flash flood susceptibility assessment using the parameters of drainage basin morphometry in SE Bangladesh. *Quatern Int* 575–576, 295–307. <https://doi.org/10.1016/j.quaint.2020.04.047>
- Aydi A, Abichou T, Nasr IH, Louati M, Zairi M (2016) Assessment of land suitability for olive mill wastewater disposal site selection by integrating fuzzy logic, AHP, and WLC in a GIS. *Environ Monit Assess* 188(1):59. <https://doi.org/10.1007/s10661-015-5076-3>
- Ayu Purnamasari R, Noguchi R, Ahamed T (2019) Land suitability assessments for yield prediction of cassava using geospatial fuzzy expert systems and remote sensing. *Comput Electron Agric* 166:105018. <https://doi.org/10.1016/j.compag.2019.105018>
- Begum F, de Bruyn LL, Kristiansen P, Islam MA (2022) Forest co-management in the Sundarban mangrove forest: Impacts of women's participation on their livelihoods and sustainable forest resource conservation. *Environ Dev* 43. <https://doi.org/10.1016/j.envdev.2022.100731>
- Béland M, Goïta K, Bonn F, Pham TTH (2006) Assessment of land-cover changes related to shrimp aquaculture using remote sensing data: a case study in the Giao Thuy District, Vietnam. *Int J Remote Sens* 27(8):1491–1510. <https://doi.org/10.1080/0143160500406888>
- Bhargava R, Sarkar D, Friess DA (2021) A cloud computing-based approach to mapping mangrove erosion and progradation: case studies from the Sundarbans and French Guiana. *Estuar Coast Shelf Sci* 248:106798. <https://doi.org/10.1016/j.ecss.2020.106798>
- Billah M, Islam AS, Mamoon WB, Rahman MR (2023) Random forest classifications for land use mapping to assess rapid flood damage using sentinel-1 and sentinel-2 data. *Remote Sens Appl: Soc Environ* 30. <https://doi.org/10.1016/j.rsap.2023.100947>
- Bunting P, Rosenqvist A, Lucas RM, Rebelo LM, Hilarides L, Thomas N, Hardy A, Itoh T, Shimada M, Finlayson CM (2018) The global mangrove watch - a new 2010 global baseline of mangrove extent. *Remote Sens* 10(10):1–19. <https://doi.org/10.3390/rs10101669>
- Center for Environmental and Geographic Information Services, CEGIS (2007) Effect of cyclone sidr on the sundarbans: a preliminary assessment. Available online: http://www.lcgbangladesh.org/derweb/cyclone/cyclone_assessment/effect%20of%20cyclone%20sidr%20on%20sundarbans_cegis.pdf (Accessed on 23 October 2021)
- Chowdhury MS, Hafsa B (2022) Multi-decadal land cover change analysis over Sundarbans Mangrove Forest of Bangladesh: a GIS and remote sensing-based approach. *Global Ecol Conserv* 37. <https://doi.org/10.1016/j.gecco.2022.e02151>
- CHRS (2020) The Center for hydrometeorology and remote sensing. Available online: www.chrsdata.eng.uci.edu (accessed on 20 Jan 2023)
- Dalagnol R, Wagner F, Lênio S, Galvão, Dutra D, Osborn B, Bientaiteur L, da P, Payne MJ, Silva C, de Favrichon S, Anderson V, Oliveira LO, Fensholt ER, Brandt M, Ciais P, Saatchi S (2023) Mapping tropical forest degradation with deep learning and planet NICFI data. *Remote Sens Environ* 298:113798–113798. <https://doi.org/10.1016/j.rse.2023.113798>
- Dasgupta S, Sobhan I, Wheeler D (2017) The impact of climate change and aquatic salinization on mangrove species in the Bangladesh Sundarbans. *Ambio* 46(6):680–694. <https://doi.org/10.1007/s13280-017-0911-0>
- Dutta AK, Pradhan P, Basu SK, Acharya K (2013) Macrofungal diversity and ecology of the mangrove ecosystem in the Indian part of Sundarbans. *Biodiversity* 14:196–206. <https://doi.org/10.1080/14888386.2013.848824>

- ESRI (2016) Arithmetic Function. Available online: <https://desktop.arcgis.com/en/arcmap/10.3/manage-data/rasterandimages/arithmetic-function.htm>. Accessed 10 Jul 2023
- Faruque MJ, Vekerdy Z, Hasan MY, Islam KZ, Young B, Ahmed MT, Monir MU, Shovon SM, Kakon JF, Kundu P (2022) Monitoring of land use and land cover changes by using remote sensing and GIS techniques in human-induced mangrove forest areas in Bangladesh. *Remote Sens Appl: Soc Environ* 25:1–14. <https://doi.org/10.1016/j.rsase.2022.100699>
- Giri C, Long J, Abbas S, Murali RM, Qamer FM, Pengra B, Thau D (2015) Distribution and dynamics of mangrove forests of South Asia. *J Environ Manage* 148:101–111. <https://doi.org/10.1016/j.jenvman.2014.01.020>
- Global Wind Atlas (2022) The global wind atlas. Available online: <https://globalwindatlas.info/en/> (accessed on 20 Jan 2023)
- Habib W, Connolly J (2023) A national-scale assessment of land use change in peatlands between 1989 and 2020 using Landsat data and Google Earth Engine—a case study of Ireland. *Reg Environ Change* 23:124. <https://doi.org/10.1007/s10113-023-02116-0>
- Halder S, Samanta K, Das S (2020) Monitoring and prediction of dynamics in Sundarban Forest using CA–Markov Chain Model. *Environ Sci Eng* 425–438. https://doi.org/10.1007/978-3-030-56542-8_18.
- Han C, Zhang Y, Shen J (2022) Fuzzy-based ecological vulnerability Assessment Driven by Human impacts in China. *Sustainability* 14(15):9166. <https://doi.org/10.3390/su14159166>
- HDX (2021) Humanitarian data exchange: bangladesh - hazards (Drought risk, Earthquake risk, Flood risk and River erosion risk). Available online: <https://data.humdata.org/dataset/bangladesh-hazards> (accessed on 22 Jan 2023)
- Hoque AF, Datta DK (2005) The mangroves of Bangladesh. *Int J Ecol Environ Sci* 31(3):245–253
- Hoque MZ, Cui S, Xu L, Islam I, Tang J, Ding S (2019) Assessing Agricultural Livelihood vulnerability to Climate Change in Coastal Bangladesh. *Int J Environ Res Public Health* 16(22):4552. <https://doi.org/10.3390/ijerph16224552>
- Hoque MA-A, Ahmed N, Pradhan B, Roy S (2019) Assessment of coastal vulnerability to multi-hazardous events using geospatial techniques along the eastern coast of Bangladesh. *Ocean Coast Manag* 181:104898. <https://doi.org/10.1016/j.occecoaman.2019.104898>
- Hoque MZ, Cui S, Islam I, Xu L, Tang J (2020) Future impact of Land Use/Land Cover Changes on Ecosystem Services in the Lower Meghna River Estuary. *Bangladesh Sustain* 12:2112. <https://doi.org/10.3390/su12052112>
- Hossain KA, Masiero M, Pirotti F (2022) Land cover change across 45 years in the world's largest mangrove forest (Sundarbans): the contribution of remote sensing in forest monitoring. *Eur J Remote Sens* 1–18. <https://doi.org/10.1080/22797254.2022.2097450>
- Ishtiaque A, Chhetri N (2016) Competing policies to protect mangrove forest: a case from Bangladesh. *Environ Dev* 19:75–83. <https://doi.org/10.1016/j.envdev.2016.06.006>
- Islam SMIDU, Bhuiyan MAH (2018) Sundarbans mangrove forest of Bangladesh: causes of degradation and sustainable management options. *Environ Sustain* 1:113–131. <https://doi.org/10.1007/s42398-018-0018-y>
- Islam M, Hossain M, Murshed S (2015) Assessment of Coastal Vulnerability due to Sea Level Change at Bhola Island, Bangladesh: using Geospatial techniques. *J Indian Soc Remote Sens* 43:625–637. <https://doi.org/10.1007/s12524-014-0426-0>
- Islam MR, Miah MG, Inoue Y (2016) Analysis of land use and land cover changes in the coastal area of Bangladesh using Landsat Imagery. *Land Degrad Dev* 27(4):899–909. <https://doi.org/10.1002/lrd.2339>
- Islam MA, Mitra D, Dewan A, Akhter SH (2016) Coastal multi-hazard vulnerability assessment along the Ganges deltaic coast of Bangladesh—A geospatial approach. *Ocean Coast Manag* 127:1–15. <https://doi.org/10.1016/j.occecoaman.2016.03.012>
- Islam MM, Borgqvist H, Kumar L (2019) Monitoring Mangrove Forest landcover changes in the coastline of Bangladesh from 1976 to 2015. *Geocarto Int* 34(13):1458–1476. <https://doi.org/10.1080/10106049.2018.1489423>
- Islam MM, Ujiie K, Noguchi R, Ahamed T (2022) Flash flood-induced vulnerability and need assessment of wetlands using remote sensing, GIS, and econometric models. *Remote Sens Appl Soc Environ* 25. <https://doi.org/10.1016/j.rsase.2021.100692>
- Jenks GF (1967) The data model concept in statistical mapping. *Int Yearb Cartogr* 7:186–190
- Jenks GF, Caspall FC (1971) Error on choroplethic maps: definition, measurement, reduction. *Ann Assoc Am Geogr* 61:217–244. <https://doi.org/10.1111/j.1467-8306.1971.tb00779.x>
- Karim MF, Zhang X, Li R (2019) Dynamics of Shrimp Farming in the Southwestern Coastal districts of Bangladesh using a shrimp yield dataset (SYD) and Landsat Satellite archives. *Sustainability* 11(17):4635. <https://doi.org/10.3390/su11174635>
- Khan AR, Khan A, Masud S, Rahman RM (2021) Analyzing the land cover change and degradation in sundarbans mangrove forest using machine learning and remote sensing technique. *Adv Comput Intell* 429–438. https://doi.org/10.1007/978-3-030-85099-9_35
- Mahmood R, Ahmed N, Zhang L, Li G (2020) Coastal vulnerability assessment of Meghna estuary of Bangladesh using integrated geospatial techniques. *Int J Disaster Risk Reduc* 42:101374. <https://doi.org/10.1016/j.ijdrr.2019.101374>
- Mahmood H, Ahmed M, Islam T, Uddin MZ, Ahmed ZU, Saha C (2021) Paradigm shift in the management of the Sundarbans mangrove forest of Bangladesh: Issues and challenges. *Trees Forests and People* 5:100094. <https://doi.org/10.1016/j.tfp.2021.100094>
- McGranahan G, Balk D, Anderson B (2007) The rising tide: assessing the risks of climate change and human settlements in low elevation coastal zones. *Environ Urbanizat* 19(1):17–37. <https://doi.org/10.1177/0956247807076960>
- McKee KL (2004) Global change impacts on mangrove ecosystems. *Fact Sheet/*. <https://doi.org/10.3133/fs20043125>
- Mondal P, Liu X, Fatoyinbo TE, Lagomasino D (2019) Evaluating Combinations of Sentinel-2 Data and Machine-Learning Algorithms for Mangrove Mapping in West Africa. *Remote Sens* 11(24):2928. <https://doi.org/10.3390/rs11242928>. MDPI AG
- Mondal B, Roy A, Saha AK (2022) Vulnerability assessment of mangrove areas in coastal West Bengal, India. *Remote Sens Appl: Soc Environ* 25. <https://doi.org/10.1016/j.rsase.2021.100680>
- Mukherjee D, Ashis KP (2021) Mangrove sensitivities to climate change and its impacts in the Sundarbans: a case study in the Patitania Island of south western Sundarbans, India. *Mod Cartogr* 353–385. <https://doi.org/10.1016/b978-0-12-823895-0.00030-0>
- Murali RM, Ankita M, Amrita S, Vethamony P (2013) Coastal vulnerability assessment of Puducherry coast, India, using the analytical hierarchical process. *Nat Nat Hazards Earth Syst Sci* 13(12):3291–3311. <https://doi.org/10.5194/nhess-13-3291-2013>
- Murshed S, Griffin AL, Islam MA, Wang XH, Paull D (2022) Assessing multi-climate-hazard threat in the coastal region of Bangladesh by combining influential environmental and anthropogenic factors. *Progress Disaster Sci* 16:100261. <https://doi.org/10.1016/j.pdisas.2022.100261>
- Muttitanon W, Tripathi NK (2005) Land use/land cover changes in the coastal zone of Ban Don Bay, Thailand using landsat 5 TM data.

- Int J Remote Sens 26(11):2311–2323. <https://doi.org/10.1080/0143116051233132666>
- Nguyen TTX, Bonetti J, Rogers K, Woodroffe CD (2016) Indicator-based assessment of climate-change impacts on coasts: a review of concepts, methodological approaches, and vulnerability indices. *Ocean Coastal Manage* 123:18–43. <https://doi.org/10.1016/j.ocecoaman.2015.11.022>
- Nikolova V, Zlateva P (2017) Assessment of Flood vulnerability using fuzzy logic and geographical Information systems. In: Murayama Y, Velev D, Zlateva P, Gonzalez J (eds) *Information Technology in Disaster Risk reduction*. ITDRR 2016. IFIP Advances in Information and Communication Technology, vol 501. Springer, Cham. https://doi.org/10.1007/978-3-319-68486-4_20
- Pastor-Guzman J, Dash J, Atkinson PM (2018) Remote sensing of mangrove forest phenology and its environmental drivers. *Remote Sens Environ* 205:71–84. <https://doi.org/10.1016/j.rse.2017.11.009>
- PDO-ICZMP (2004) Living in the coast problems, opportunities and challenges. Program Development Office for Integrated Coastal Zone Management Plan
- Prabakaran N, Bayyana S, Vetter K et al (2021) Mangrove recovery in the Nicobar archipelago after the 2004 tsunami and coastal subsidence. *Reg Environ Change* 21:87. <https://doi.org/10.1007/s10113-021-01811-0>
- Quader MA, Agrawal S, Kervyn M (2017) Multi-decadal land cover evolution in the Sundarbans, the largest mangrove forest in the world. *Ocean Coastal Manage* 139:113–124. <https://doi.org/10.1016/j.ocecoaman.2017.02.008>
- Ramakrishnan R, Gladston Y, Kumar NL et al (2020) Impact of 2004 co-seismic coastal uplift on the mangrove cover along the North Andaman Islands. *Reg Environ Change* 20:6. <https://doi.org/10.1007/s10113-020-01608-7>
- Rehman S, Sahana M, Kumar P et al (2021) Assessing hazards induced vulnerability in coastal districts of India using site-specific indicators: an integrated approach. *GeoJournal* 86:2245–2266. <https://doi.org/10.1007/s10708-020-10187-3>
- Roy DAKD, Gow J (2015) Attitudes towards current and alternative management of the Sundarbans Mangrove Forest, Bangladesh, to achieve sustainability. *J Environ Plann Manage* 58(2):213–228. <https://doi.org/10.1080/09640568.2013.850405>
- Roy K, Gain AK, Mallick B, Vogt J (2017) Social, hydro-ecological, and climatic change in the southwest coastal region of Bangladesh. *Reg Environ Change* 17:1895–1906. <https://doi.org/10.1007/s10113-017-1158-9>
- Roy B, Penha-Lopes GP, Uddin MS, Kabir MH, Lourenço TC, Torrejano A (2022) Sea level rise induced impacts on coastal areas of Bangladesh and local-led community-based adaptation. *Int J Disaster Risk Reduct* 73:102905. <https://doi.org/10.1016/j.ijdr.2022.102905>
- Sahoo B, Bhaskaran PK (2018) Multi-hazard risk assessment of coastal vulnerability from tropical cyclones - a GIS based approach for the Odisha coast. *J Environ Manage* 206:1166–1178. <https://doi.org/10.1016/j.jenvman.2017.10.075>
- Seyam MMH, Haque MR, Rahman MM (2023) Identifying the land use land cover (LULC) changes using remote sensing and GIS approach: a case study at Bhaluka in Mymensingh, Bangladesh. *Case Stud Chem Environ Eng* 7. <https://doi.org/10.1016/j.cscee.2022.100293>
- Simon O, Lyimo J, Yamungu N (2023) Land use and cover change in Dar Es Salaam metropolitan city: satellite data and CA-Markov chain analysis. *Geo Journal*. <https://doi.org/10.1007/s10708-023-10960-0>
- Singh M, Schwendenmann L, Wang G, Adame MF, Mandlak LJC (2022) Changes in Mangrove Carbon stocks and exposure to sea level rise (SLR) under future climate scenarios. *Sustainability* 14(7):3873. <https://doi.org/10.3390/su14073873>
- SRTM, USGS (2023) Shuttle Radar Topography Mission (SRTM), The United States Geological Survey. Available online: <https://earthexplorer.usgs.gov/>. Accessed on 27 Jan 2023
- Subramanian A, Nagarajan AM, Vinod S, Chakraborty S, Sivagami K, Theodore T, Sathyarayanan SS, Tamizhdurai P, Mangesh VL (2023) Long-term impacts of climate change on coastal and transitional eco-systems in India: an overview of its current status, future projections, solutions, and policies. *RSC Adv* 13(18):12204–12228. <https://doi.org/10.1039/d2ra07448f>
- Sun X, Crittenden J, Li F, Lu Z, Dou X (2018) Urban expansion simulation and the spatiotemporal changes of ecosystem services, a case study in Atlanta Metropolitan area, USA. *Sci Total Environ* 622:623. <https://doi.org/10.1016/j.scitotenv.2017.12.062>
- Swain S, Mishra SK, Pandey A et al (2022) Inclusion of groundwater and socio-economic factors for assessing comprehensive drought vulnerability over Narmada River Basin, India: a geo-spatial approach. *Appl Water Sci* 12(14). <https://doi.org/10.1007/s13201-021-01529-8>
- USGS (2021) The United States Geological Survey. Available online: <https://earthexplorer.usgs.gov/>. Accessed on 27 Jan 2023
- Wang L, Jia M, Yin D, Tian J (2019) A review of remote sensing for mangrove forests: 1956–2018. *Remote Sens Environ* 231:111223. <https://doi.org/10.1016/j.rse.2019.111223>
- WorldPop (2015) Bangladesh - Population density. Available online: <https://energydata.info/dataset/bangladesh--population-density-2015>. Accessed on 12 Jan 2023
- Worthington TA, Andradi-Brown DA, Bhargava R, Buelow C, Bunting P, Duncan C, Fatoyinbo L, Friess DA, Goldberg L, Hilarides L, Lagomasino D, Landis E, Longley-Wood K, Lovelock CE, Murray NJ, Narayan S, Rosenqvist A, Sievers M, Simard M, Thomas N (2020) Harnessing Big Data to Support the Conservation and Rehabilitation of Mangrove forests globally. *One Earth* 2(5):429–443. <https://doi.org/10.1016/j.oneear.2020.04.018>
- Yirsaw E, Wu W, Shi X, Temesgen H, Bekele B (2017) Land Use/Land Cover Change modeling and the prediction of subsequent changes in Ecosystem Service values in a Coastal Area of China, the Su-Xi-Chang Region. *Sustainability* 9(7):1204. <https://doi.org/10.3390/su9071204>

Publisher's Note Springer Nature remains neutral with regard to jurisdictional claims in published maps and institutional affiliations.